Food Research International 172 (2023) 113180

Contents lists available at ScienceDirect

Food Research International

journal homepage: www.elsevier.com/locate/foodres

Quantifying the effects of pre-roasting on structural and functional properties of yellow pea proteins

Yanyan Lao [a], Qianyu Ye [a], Yong Wang [a], Jitraporn Vongsvivut [b], Cordelia Selomulya [a,*]

[a] School of Chemical Engineering, UNSW Sydney, Kensington, NSW 2052, Australia
[b] Infrared Microspectroscopy Beamline, ANSTO Australian Synchrotron, Clayton, Victoria 3168, Australia

ARTICLE INFO

Keywords:
Pea protein
Extraction
Roasting
Solubility
Protein structure
Functionality

ABSTRACT

Roasting could modify the protein structure/conformation, contributing to changes in functional properties. Here we investigated the effects of pre-roasting on the extraction efficiency, structural and functional properties of pea protein concentrates and isolates (PPC and PPI) produced from yellow split peas. The shorter roasting times (150 °C, 10 and 20 min) had little effect on protein yields and could increase the solubility of PPC or PPI by ~ 12% at pH 7 and enhance the solubility of PPI by ~ 12% (10-min roasting) and ~ 24% (20-min roasting) at pH 3. However, a longer duration of pre-roasting (150 °C, 30 min) significantly reduced the extraction efficiency of PPC and PPI by ~ 30% and ~ 61%, respectively. Meanwhile, pre-roasting had minor effects on SDS-PAGE profiles and the secondary structures of pea proteins but significantly altered tertiary structures by reducing free sulfhydryl groups, increasing disulfide bonds and surface hydrophobicity. As for the emulsifying properties, pre-roasting improved the emulsion ability index (EAI) of PPC and PPI but decreased the emulsion stability index (ESI) of PPC and had no significant effect on PPI. Moreover, PPC and PPI with shorter pre-roasting duration (10 and 20 min) had endothermic peaks and showed a slight decrease in the denaturation temperature (T_d) and the onset temperature (T_o), respectively. Overall, the study demonstrated that controlled pre-roasting at 150 °C for 10 min and 20 min altered protein structures (mainly tertiary structures), improving the solubility and EAI of pea proteins at pH 7, while retaining their thermal properties in comparison to unroasted samples.

1. Introduction

The utilization of plant proteins has gathered significant attention because of their perceived sustainability and health benefits. Soy protein has emerged as the leading ingredient in plant-based food formulation (Vallath et al., 2022), with a market value of USD 7.2 billion in 2021 and a compound annual growth rate (CAGR) of 7.0%. Soy protein holds a market share that is more than four times that of other mainstream plant proteins such as pea and wheat proteins in Asia Pacific (Markets, 2022). However, concerns over genetically modified soybeans and soy protein allergies have led to an increased demand for alternative plant-based protein sources. Pea protein, derived from yellow peas, could be an ideal alternative to soy protein due to its hypoallergenic, non-transgenic status and sufficient essential amino acid content (Boukid et al., 2021; Gorissen et al., 2018). From a cost perspective, pea protein is almost half the price of milk protein and a quarter less than soy protein (Kent & Doherty, 2014). Nevertheless, the low solubility of pea protein limits its application as an ingredient or a functional component in the food system. The solubility of commercially available pea protein isolate (PPI) (Bulk Nutrients, Tasmania, Australia) measured in our preliminary experiment was only 16.8 ± 2.8% (w/v) at pH 7 (unpublished data). Tanger et al. (2020) and Jiang et al. (2017) also found low solubility (<20%, w/v) across a pH range of 3–8 for commercial PPI from other suppliers. Therefore, it is necessary to seek feasible approaches to enhance the solubility of pea proteins.

Several factors affecting plant protein solubility and strategies for enhancing solubility or emulsifying properties were summarized. Firstly, a mild fractionation process can produce plant proteins with better solubility. It was reported that the isoelectric precipitation of protein may result in irreversible changes in the tertiary structure of pea globulins, which would induce aggregation and hydrophobic interaction and reduce solubility (Kornet et al., 2020). The extraction of pea protein concentrate (PPC) only involved a dissolution step, resulting in higher solubility compared to PPI with further precipitation at the isoelectric point (Kornet et al., 2020). Diafiltration as a mild purification method could retain both globulins and hydrophilic albumins of PPI, and its

* Corresponding author.
E-mail address: cordelia.selomulya@unsw.edu.au (C. Selomulya).

https://doi.org/10.1016/j.foodres.2023.113180
Received 14 April 2023; Received in revised form 18 June 2023; Accepted 19 June 2023
Available online 20 June 2023

solubility was higher by 18.4% than that of PPI extracted by isoelectric precipitation with albumin removed (Kornet et al., 2021a). Moreover, Kornet et al. (2022) found that the mildly purified PPC and highly purified PPI showed comparable emulsifying properties at a low concentration (0.7% wt) since globulins in PPC had sufficient capability to stabilise emulsions. However, PPC contains more oligosaccharides and anti-nutritional factors than PPI (Kornet et al., 2020), which may cause flatulence and gastrointestinal discomfort. The scale of the processing batch was shown to influence the solubility and emulsification of pea proteins. Burger et al. (2022) reported that the solubility of pea protein prepared on a laboratory scale was 10% (w/v) higher than that prepared on a pilot scale at pH 7, and the protein produced in the smaller batch scale could form more stable emulsions with smaller droplet sizes. Several techniques such as chemical, physical, and enzymatic modifications are promising ways to improve the solubility and functionality of pea proteins (Sharif et al., 2018). Nevertheless, chemical modification may introduce synthetic chemical components (Shen et al., 2022). Physical modifications such as ultrasonic, high-pressure homogenization, and high hydrostatic pressure treatments require expensive equipment, while the cost of enzymatic treatment is high (Fang et al., 2020). Thus, these methods may have some limitations for the scale-up production of plant proteins. Heat treatment presented the potential to facilitate protein solubility if the conditions were carefully controlled, and thermal treatment can be readily applied to large-scale production (Yang et al., 2022a). Spray drying and freeze drying are often used for protein powders production, and their effects on protein solubility are related to the extraction methods and drying conditions (Burger et al., 2022; Yang et al., 2022a).

Roasting is a common pre-treatment method for plant seeds before milling. Some studies have shown that moderate roasting had a positive effect on protein solubility and emulsification. Ma et al. (2011) reported that roasted pea flour (roasted at 80 °C for 1 min) had higher protein solubility and emulsifying properties than unroasted one at pH 7. The solubility alteration may be caused by intramolecular hydrogen bonds, disulfide-sulfhydryl interchange reactions, and isoelectric point acid shifting during heating, with a diverse degree of biochemical changes in protein structure, leading to different solubility and functionality changes (Ma et al., 2011; Neucere, 1972). Stone et al. (2021) found that wet roasting (roasting at 160 °C for 30 min after tempering pea seeds to 20% or 30%) enabled to improve in the oil-holding capacity of yellow pea flour since roasting enhanced the exposed hydrophobic groups of proteins. Additionally, roasted plant seeds can be ground into powder for protein extraction. For instance, the solubility and emulsion stability index of peanut protein isolate extracted from roasted peanut (225 °C for 25 min) were improved by 12.6% and 27.0%, respectively, because the Maillard reaction during roasting changed the major cytoplasmic globulin of peanut (Zaaboul et al., 2019). It is worth noting that roasting conditions (temperature/time) have a notable impact on protein solubility due to the different degrees of denaturation and modification in protein structure. Mesfin et al. (2021) indicated that roasting chickpea flour at 150 °C for 30 min increased the solubility of protein by more than 10%, while roasting at 180 °C for 15 min resulted in much lower solubility.

Although roasting treatment may improve protein functionality, to the best of our knowledge no systematic studies on the impact of roasting before extraction (pre-roasting) on the extraction efficiency of pea proteins and their functional properties have been reported. This study aims to investigate the effect of roasting pre-treatment on the extraction efficiency and physicochemical functionalities (solubility, emulsifying, and thermal properties) of pea proteins for their potential application in plant-based milk formulations.

2. Materials and methods

2.1. Materials

Yellow split peas (Ward McKenzie Pty. Ltd., Victoria, Australia) and commercial pea protein isolate (Bulk Nutrients, Tasmania, Australia) were bought from a local supermarket (Sydney, Australia). Quick Start Bradford 1 × Dye Reagent, 2 × Laemmli Sample Buffer, 2-mercaptoethanol, Precision Plus Protein Dual Xtra Standards, 4–15% Mini-PROTEAN TGX Precast protein gels, 10 × Tris/Glycine/SDS, Coomassie Brilliant Blue R-250 stain were purchased from Bio-Rad (Hercules, California, USA). The other reagents were purchased from Sigma-Aldrich (St. Louis, Missouri, USA) and Chemsupply (Gillman, South Australia) unless otherwise specified.

2.2. Methods

2.2.1. The pre-treatment of pea seeds

Commercial yellow split peas were roasted at 150 °C for 10, 20, and 30 min in a compact oven (Smeg Pty. Ltd., Guastalla, Italy) in a static mode. Once cooled, the roasted pea seeds were milled with a high-speed blender (Optimum G2.6 Platinum Series; Optimum Appliances Pty. Ltd., Victoria, Australia) in a dry grind mode for 70 s. The obtained pea flour was sifted with a 100-μm sieve (Endecotts Ltd., London, England) for subsequent protein extraction. Proteins extracted from unroasted pea flour were used as control samples.

2.2.2. Pea protein aqueous extraction

Different pea protein powders extracted from unroasted or roasted pea seeds were obtained using the method reported by Kornet et al. (2020) with minor modifications. Two types of pea proteins with different protein contents (different purities) were extracted (Fig. 1), namely pea protein concentrate (PPC) and pea protein isolate (PPI). Here, we applied freeze drying to obtain the protein powders, as thermal drying methods like spray drying would introduce extra heat stress, which may render it difficult to differentiate whether the change in protein properties was caused by roasting or the thermal drying process. The specific steps were described in Supplementary Material (Method 1). The extraction process was repeated twice. Key extraction conditions of eight samples were listed in **Table S1** and the yield of protein was calculated by **Equation (1)**:

$$Yield(\%) = \frac{The\ weight\ of\ obtained\ protein\ powder(g)}{The\ weight\ of\ initial\ pea\ flour(g)} \times 100\% \quad (1)$$

2.2.3. Total/soluble protein content and protein solubility

Total protein content was calculated from the nitrogen content with a conversion factor of 6.25 (Mession et al., 2013). Specifically, 20–30 mg of samples were combusted at 1150 °C in a varioMACRO cube (Langenselbold, Germany), and the resulting N-related gases were checked and analysed to get the total nitrogen content. Protein recovery (%) was expressed as the percentage of total protein content in extracted protein to that of corresponding pea flour.

Pea protein samples (20 mg) were dissolved in 10 mL Milli-Q water, followed by adjusting the pH value of suspensions to 3, 4, 5, 6, 7, and 8 using 0.1 M NaOH or HCl and shaking at 200 rpm for 2 h at room temperature (Bioline shaker BL8600; Bioline Global Pty Ltd., UK). Then, all suspensions were centrifuged at 10,000 × g for 20 min at 20 °C to separate the non-soluble parts. The supernatants were used to determine soluble protein content with the Bradford method (Bradford, 1976). The specific method was described in Supplementary Material (Method 2). The protein solubility can be calculated by **Equations (2) (3)**:

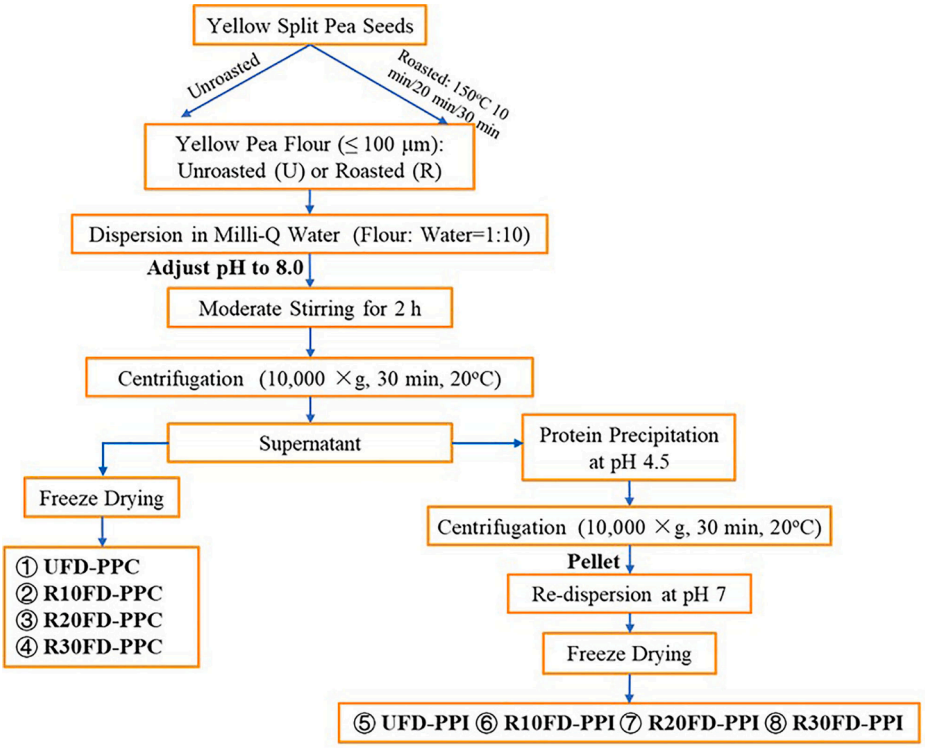

Fig. 1. Flow chart of extracting pea protein concentrates (PPC) and pea protein isolates (PPI) using unroasted and roasted pea seeds. (U: unroasted; R: roasted; R10, R20, R30: pea seeds roasted at 150 °C for 10, 20 and 30 min, respectively; FD: freeze drying).

$$Soluble\ protein\ content\ (\%, w/v) = \frac{Soluble\ protein\ concentration\ (\mu g/mL)}{Original\ protein\ powders\ concentration (\mu g/mL)} \times 100\% \quad (2)$$

$$Protein\ solubility\ (\%, w/v) = \frac{Soluble\ protein\ content\ (\%)}{Total\ protein\ content\ in\ pea\ protein\ powders\ (\%)} \times 100\% \quad (3)$$

2.2.4. Total carbohydrates, starch, and ash content

Total carbohydrates were determined by the phenol–sulfuric acid method described by Masuko et al. (2005) with minor modification, expressing as the percentage (wt%) of equivalent glucose. Starch content was analysed based on the amyloglucosidase-hexokinase-glucose 6-phosphate dehydrogenase enzymatic method by a starch assay kit from Sigma (St. Louis, Missouri, USA). Ash content was determined by heating samples at 600 °C for 2 h in a Nabertherm furnace (Lilienthal, Germany) according to AOAC method 942.05. All measurements were conducted in duplicate. The detailed determination methods were described in Supplementary Material (Method 3).

2.2.5. Colour measurement and sample pictures

The colour characteristic of protein samples was indicated by L^* (lightness), a^* (redness), and b^* (yellowness) values. A colourimeter (HunterLab, ColorQuest XE, Reston, USA) equipped with a 0.375-inch sensor view area was used. The instrument was calibrated with a white standard plate before testing. Each sample was finely ground with a mortar and placed in identical transparent packaging and measured in reflectance mode. Five measurements were taken for each sample. Images of different proteins were captured using a camera (Nikon, D5600). To ensure a consistent ambient brightness, the samples were placed in a light box, with the distance between the lens and the samples set at 35 cm, and the light sensitivity (ISO) value was 640.

2.2.6. Sodium dodecyl sulfate–polyacrylamide gel electrophoresis (SDS-PAGE)

SDS-PAGE of pea proteins was performed based on the methodology of Kim et al. (2022) and Gao et al. (2020) with minor modifications. 30 mg protein powders were dissolved in 10 mL of PBS buffer (0.01 M, pH 7) and shaken at 200 rpm for 2 h at room temperature. The insoluble part of proteins was removed by centrifuging at 10,000 × g for 20 min at 20 °C. The obtained protein solution was used for non-reducing and reducing SDS-PAGE analysis. The detailed steps were presented in Supplementary Material (Method 4).

2.2.7. Fourier transform infrared (FT-IR) spectroscopy

The FT-IR spectra of pea proteins were performed with Bruker Alpha (BRKR, Massachusetts, USA) with attenuated total reflection (ATR) accessory. The detailed steps were recorded in Supplementary Material (Method 5). OMNIC 32 software (Thermo Fisher Scientific, MA, USA) was used to collect peaks of spectra. The secondary structure was analysed using Peakfit software (Systat Software, Inc. USA) through Gaussian deconvolution and second derivative spectra fitting in the region of amide I 1700-1600 cm^{-1} (Kong & Yu, 2007). The peak assignment of the secondary structures is as follows: intermolecular (hydrogen-bonded) β-sheet (~1682 and ~ 1619 cm^{-1}), native β-sheet (1640-1630 cm^{-1}), β-turn (~1673 cm^{-1}), α-helix (~1654 cm^{-1}), random coil (~1645 cm^{-1}) (Carbonaro et al., 2012; Meng & Ma, 2001; Zandomeneghi et al., 2004).

2.2.8. Surface hydrophobicity

Surface hydrophobicity (*Ho*) was measured according to the method of Jiang et al. (2017) and Shen et al. (2021) with slight modifications. 8 mM ANS stock solution was prepared in phosphate buffer (PBS, 0.01 M, pH 7) and used as the fluorescence probe. Four protein concentrations, from 0.005% to 0.04 % (w/v), were prepared with the same PBS buffer (0.01 M, pH 7). The preparation method for the protein solution was the same as that in section 2.2.6. The specific steps were covered in the Supplementary Material (Method 6).

2.2.9. Sulfhydryl group (SH) and disulfide bond (SS) contents

The contents of total SH, free SH, and SS were measured according to Cui et al. (2020) with minor modifications. The detailed measurement steps were covered in Supplementary Material (Method 7).

2.2.10. Zeta potential and mean particle size

The zeta potential of protein solutions was measured with a Zetasizer (Zetasizer Nano ZS, Malvern Panalytical Instrumentation, UK) according to the method described by Yang et al. (2022a) with minor modifications. 0.2% (w/v) protein suspensions were prepared in Milli-Q water, followed by adjusting the pH value to 3, 4, 5, 6, 7, and 8. After the suspensions were mixed at 200 rpm and incubated at room temperature for 2 h, centrifugation (10,000*g*, 20 min, 20 °C) was performed to obtain the protein supernatant. All samples were placed into a capillary zeta cell (DTS1070) to conduct the zeta potential at 25 °C. The refractive indices for proteins and the dispersant were set at 1.45 and 1.33, respectively. The mean particle sizes of samples were determined at pH 7 with the same temperature and refractive indices.

2.2.11. Emulsion ability index (EAI) and emulsion stability index (ESI)

EAI and ESI were measured according to the method of Gao et al. (2022) with some modifications. 0.1% (wt%) protein suspensions were prepared by PBS buffer (0.01 M, pH 7), shaking at 200 rpm for 2 h at room temperature (Bioline shaker BL8600; Bioline Global Pty Ltd., UK). Then, 25% (wt%) commercial sunflower oil was added (protein solution: oil = 3:1). After homogenization (15,000 rpm for 1 min) for 0 min and 10 min with a high shear homogeniser (IKA-T25 Ultra Turrax, IKA Ltd., Germany), 50 μL of the emulsion was immediately taken from the bottom of the beaker and added into 5 mL 0.1% SDS solution. The diluted emulsion was measured in the cuvette with a 1-cm optical path and the absorbance was recorded at 500 nm using Infinite 200 PRO (Tecan Trading AG, Switzerland). The EAI and ESI were calculated with **Equations (4) (5)**:

$$EAI\left(m^2/g\right) = \frac{2 \times 2.303}{10^4 \times \theta \times L \times C} \times A_0 \times DF \tag{4}$$

$$ESI(\min) = \frac{A_0}{A_0 - A_{10}} \times (T_{10} - T_0) \tag{5}$$

where DF: dilution factor (100); $T_{10} - T_0$: time duration (10 min); A_0 and A_{10}: absorbance measured at 500 nm immediately or after 10 min of emulsion formation, respectively; C: protein concentration (mg/g); θ: dispersed phase (oil) weight fraction (0.25); L: optical path (1 cm).

2.2.12. Thermal property

The onset temperature (T_o), peak temperature (T_d), and enthalpy (ΔH) of samples were collected from heat flow diagrams using TA Universal Analysis 2000 software (Yang et al., 2022a). The detailed methods were covered in Supplementary Material (Method 8).

2.3. Statistical analysis

All the experiments were performed in triplicate unless otherwise specified. Microsoft Excel was used to record the data and calculate the average and standard deviation. A 95% confidence level was used when one-way analysis of variance (ANOVA) was applied in IBM SPSS Statistics 26.0 (IBM Inc., USA) to determine the significance level of difference between the averages. Origin 2019 (OriginLab Corporation, USA) was used to plot figures.

3. Results and discussion

3.1. Extraction efficiency and solubility of pea proteins

The yield and recovery of pea proteins were measured as indicators of protein extraction efficiency (Skylas et al., 2017). As presented in Table 1, except for the protein extracted from pea seeds roasted for 30 min (R30FD-PPC/PPI) with significantly lower yields ($P < 0.05$), the pea proteins extracted with shorter roasting times (10 and 20 min) had similar yields to the proteins derived from unroasted pea flour (UFD-PPC/PPI). This may be because the longest roasting time (30 min) led to significant changes in the pH for protein dissolution and precipitation in pea flour, impairing the overall extraction efficiency (Skylas et al., 2017). Ma et al. (2011) found the secondary/tertiary structure changes of the pea protein after roasting the yellow pea flour at 80 °C for 1 min. Thus, the treatment conditions with higher temperature (150 °C) and longer time (10, 20, and 30 min) in our study were presumably able to change the protein structures. In general, pulse proteins will have a lower yield or recovery percentage when targeting higher purity (Tenorio et al., 2018), consistent with the results in this study which was showing that PPI had lower extraction efficiency than PPC (Table 1). Apart from R30FD-PPC, the total protein contents of other pea proteins extracted from roasted flours were comparable to that extracted from unroasted flour, suggesting that the methods were still effective for protein fractionation after pre-roasting.

As shown in Fig. 2 **(A1) & (A3)**, all pea proteins displayed a pH-dependent U-shaped curve of solubility with the lowest solubility at pH 4 and 5 since they were near the isoelectric point of pea proteins. The curves presented in Fig. 2 **(A2) & (A4)** demonstrated that the lowest net charge on the protein surface was in the range of pH 4–5. The solubility range of PPC samples (16.2% − 30.5%) was notably higher at pH 4 and 5 than those of PPI samples (2.0% − 10.8%), since PPC retained albumins that were soluble around the isoelectric point while PPI removed albumins after isoelectric precipitation (Yang et al., 2020). As seen in Fig. 2 **(A1)**, PPC samples extracted from roasted pea flours (RFD-PPC) presented a lower solubility than UFD-PPC at acidic condition (pH 3) but with higher solubility at pH 7, showing the same solubility pattern of pea

Table 1
The protein extraction efficiency and main composition (dry basis, wt%) of PPC and PPI with different roasting times.

Samples	Yield (%)	Protein recovery (%)	Protein (%)	Total carbohydrates (%)	Starch (%)	Ash content (%)
UFD-PPC	25.9 ± 1.3^{a}	72.3 ± 0.9^{a}	58.9 ± 0.7^{e}	16.5 ± 0.4^{d}	1.5 ± 0.0^{b}	6.2 ± 0.0^{d}
R10FD-PPC	25.4 ± 1.0^{a}	64.1 ± 0.5^{c}	60.3 ± 0.3^{d}	18.8 ± 1.9^{c}	1.6 ± 0.0^{a}	6.5 ± 0.1^{c}
R20FD-PPC	25.2 ± 0.1^{a}	66.2 ± 1.1^{b}	60.6 ± 0.2^{d}	20.5 ± 0.1^{b}	1.1 ± 0.1^{c}	7.1 ± 0.0^{b}
R30FD-PPC	18.1 ± 2.8^{b}	41.9 ± 0.5^{f}	46.8 ± 0.7^{f}	27.9 ± 0.3^{a}	1.0 ± 0.0^{d}	8.6 ± 0.1^{a}
UFD-PPI	12.0 ± 0.2^{c}	47.5 ± 0.4^{e}	85.8 ± 0.5^{c}	2.4 ± 0.1^{f}	0.1 ± 0.0^{e}	0.7 ± 0.0^{f}
R10FD-PPI	11.7 ± 0.1^{c}	49.0 ± 0.2^{d}	96.3 ± 0.8^{a}	2.8 ± 0.0^{f}	0.1 ± 0.0^{e}	0.6 ± 0.0^{f}
R20FD-PPI	11.5 ± 0.2^{c}	48.0 ± 0.9^{de}	97.0 ± 0.3^{a}	2.3 ± 0.1^{f}	0.1 ± 0.0^{e}	0.6 ± 0.0^{f}
R30FD-PPI	4.6 ± 2.2^{d}	25.2 ± 0.1^{g}	91.0 ± 0.3^{b}	4.8 ± 0.1^{e}	0.1 ± 0.0^{e}	0.9 ± 0.0^{e}

Different letters of the same column present significant differences ($P < 0.05$).

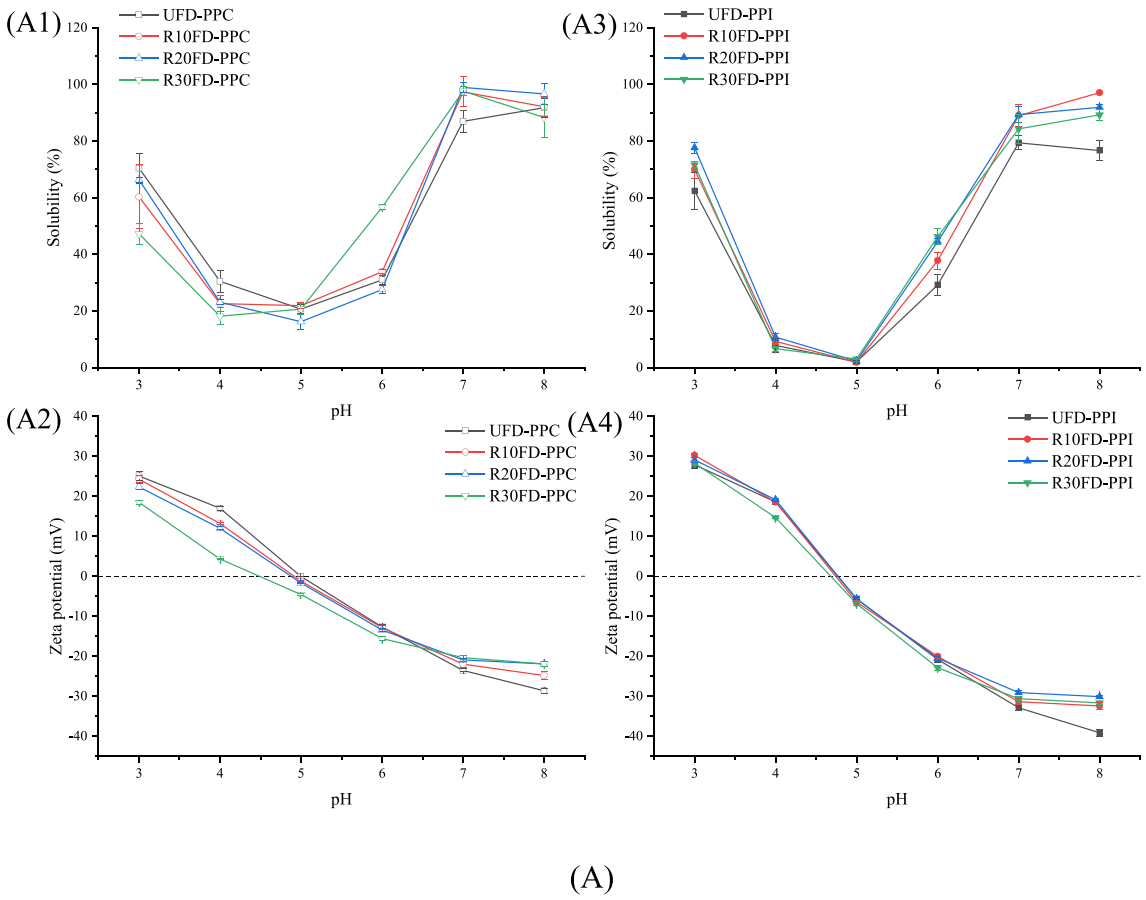

(A)

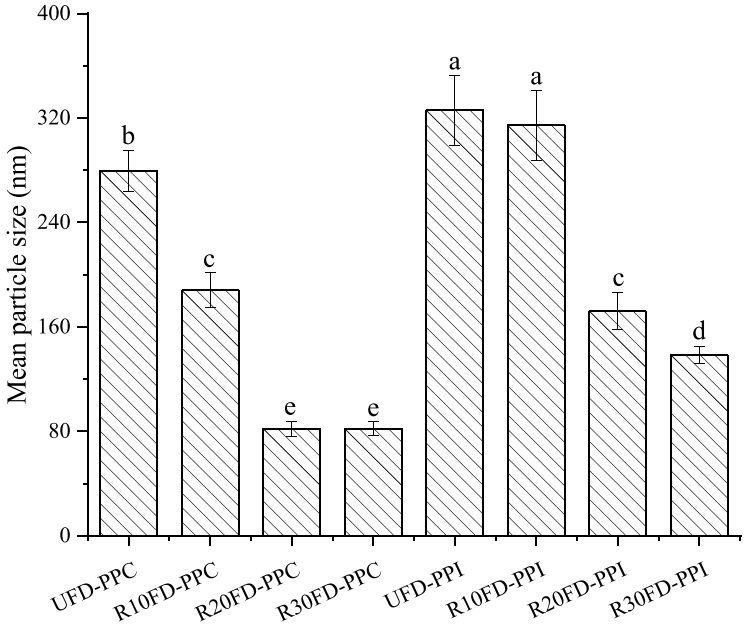

(B)

Fig. 2. **(A)** pH-dependence of pea protein solubility (%) and surface charge (zeta potential) at pH 3-8: **(A1)** Solubility (%) and **(A2)** Zeta potential of different PPC; **(A3)** Solubility (%) and **(A4)** Zeta potential of different PPI. **(B)** Effect of roasting on the mean particle size of pea proteins at pH 7. Different letters show significant differences ($P < 0.05$).

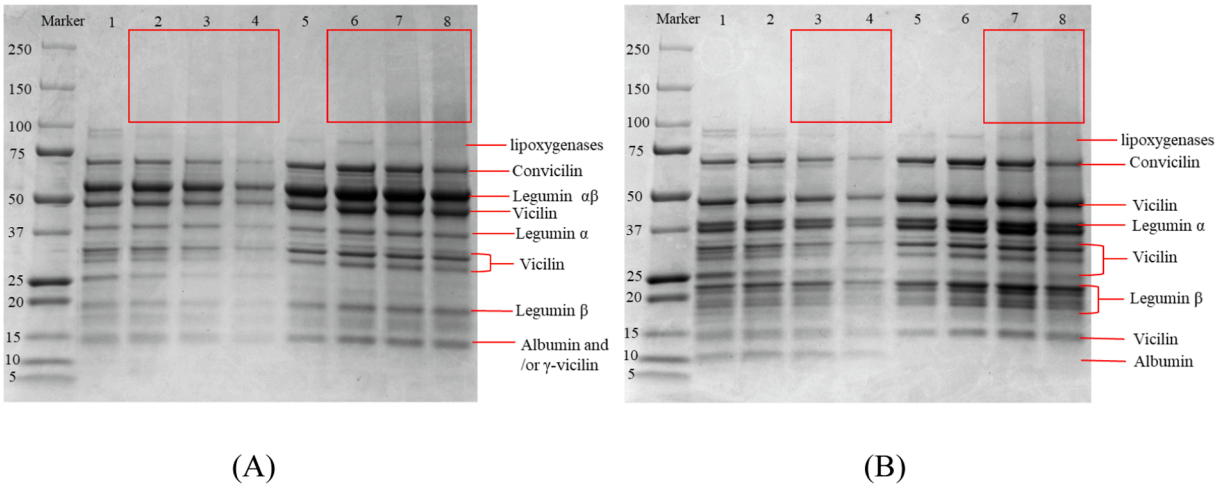

Fig. 3. Non-reducing **(A)** and reducing **(B)** SDS-PAGE profiles of different extracted pea proteins: 1. UFD-PPC, 2. R10FD-PPC, 3. R20FD-PPC, 4. R30FD-PPC, 5. UFD-PPI, 6. R10FD-PPI, 7. R20FD-PPI, 8. R30FD-PPI (Red frames indicate broad stained bands in high molecular weight). (For interpretation of the references to colour in this figure legend, the reader is referred to the web version of this article.)

proteins in pea flour as reported by Ma et al. (2011). Fig. 2 **(A2)** shows that the isoelectric point of RFD-PPC shifted to a more acidic pH (pH 5 → 4), especially for R30FD-PPC, resulting in reduced solubility under strongly acidic conditions (pH 3 and 4). In turn, when the pH is from 6 to 7, the solubility of RFD-PPC increased more significantly than UFD-PPC since roasted samples are farther away from their isoelectric point. The solubility of RFD-PPC samples decreased when pH > 7, especially R30FD-PPC, which may be due to alkaline conditions accelerating the Maillard reaction and facilitating the formation of insoluble products in RFD-PPC (Nagai et al., 1998; Yu et al., 2021). This effect was more significant in RFD-PPC than in UFD-PPC since RFD-PPC may have accumulated some reaction products from the initial stage of the Maillard reaction during pre-roasting. In contrast, all RFD-PPI presented higher solubility than the UFD-PPI when the pH was 3, 6, 7, and 8 (Fig. 2 **(A3)**). It is worth mentioning that the solubility of RFD-PPI samples even increased at strong acidic condition (pH = 3) by the range of 12% – 24%. The different solubility patterns may result from the existence of more carbohydrates in PPC than that in PPI ($P < 0.05$) (Table 1), which were prone to participate in the Maillard reactions with proteins. In addition, the PPI structure changed more significantly than PPC during further purification by isoelectric precipitation, while the structure of PPC was closer to the proteins naturally present in pea flour (Kornet et al., 2020). All RFD-PPC and RFD-PPI presented significantly higher ($P < 0.05$) solubility than the UFD-PPC/PPI at neutral pH. The solubility of RFD-PPC and RFD-PPI reached more than 95% and around 85% at pH 7, respectively, which was 12.0% – 13.7% higher than UFD-PPC, and 6.2% – 12.5% higher than UFD-PPI. That is because pH 7 was far from the isoelectric point of the proteins, reducing the possibility of protein aggregation and precipitation. Furthermore, Yang et al. (2022a) referred to the 'soluble' protein aggregates caused by heating, which had small particle sizes (0.05-0.70 μm) and can only be removed with ultracentrifugation (45 min at 320,000 × g) (Sridharan et al., 2020). The soluble aggregates, mainly legumins and vicilins (based on the protein profile of SDS-PAGE, Fig. 4), may be generated in this study, because of the lower protein particle sizes of roasted samples at pH 7 (Fig. 2 **(B)**), which cannot be separated under current centrifugation conditions (10,000 × g for 20 min).

Zeta potential represents the surface charge of proteins and is regarded as an indicator of electrostatic interactions between particles (Kornet et al., 2022). In the pH range of 3-8, protein solubility reached a maximum at pH 7-8, and the absolute values of zeta potential ($|\zeta|$) of PPC and PPI were greater than 20 mV and 30 mV, respectively. As shown in Fig. 2 **(A2)**, apart from pH 5 and 6, the $|\zeta|$ of PPC extracted from the roasted pea seeds were lower than those derived from the unroasted pea seeds, especially for R30FD-PPC. This may be because roasting triggered the glycation between proteins and carbohydrates, leading to electrostatic screening and thereby reducing the surface charges in most pH values (Kutzli et al., 2020). In comparison, the difference between RFD-PPI and UFD-PPI was much smaller than that of PPC (Fig. 2 **(A4)**), which may result from that PPI was more highly purified than PPC and contained fewer glycated components. Doan and Ghosh (2019) found that heating at 95 °C for 15 min and then cooling down to 65 °C could increase the $|\zeta|$ by ~ 20% and ~ 80% for pea protein nanoparticles at pH 3 and 10, respectively. Yang et al. (2022a) concluded that the heating process (95 °C for 5 min) of protein extracts before drying did not affect the surface charges. The contradicting results may be associated with the diverse samples and heating conditions used in those studies, as different forms of protein require specific heating energy to convert the surface structure. The above studies used protein extracts or protein solutions exposed to thermal treatment, while in our study, the thermal treatment was conducted on pea seeds, where the proteins exist as protein bodies and are protected by cell walls (Kornet et al., 2020). That is why the pea seeds could be treated at much higher temperatures than extracted proteins. All the PPI samples had higher $|\zeta|$ than PPC samples at the same pH. For example, PPI had higher surface charges (−32.9 - −29.1 mV) than their PPC counterparts (−23.6 - −20.4 mV) at pH 7. Meanwhile, the PPI samples (138.6-325.9 nm) had higher mean particle sizes than the corresponding PPC samples (82.1-279.8 nm) at a neutral condition (Fig. 2 **(B)**). This could be explained by the fact that PPC and PPI contain different protein components. Albumins that exist in PPC while mostly absent in PPI since they were lost during isoelectric precipitation had lower surface charge and smaller molecules than globulins (Kornet et al., 2020; Tanger et al., 2020). As a result, the PPC as a mixture of globulins and albumins showed smaller particle sizes and lower surface charges than PPI containing only globulins.

Overall, extracting pea proteins from pea flour roasted at 150 °C for 10 min and 20 min seems to be promising pre-treatment conditions for improving protein solubility while still maintaining the extraction efficiency.

3.2. Protein structure characterisation

3.2.1. SDS-PAGE analysis

The protein profiles of PPI and PPC were assessed using non-reducing and reducing SDS-PAGE. As shown in Fig. 3, multiple bands with molecular weights (MW) from 10 to 97 kDa and 15 to 88 kDa were exhibited in electrophoretic lanes of PPC and PPI, respectively. The light band at 90-97 kDa was attributed to lipoxygenase, which is closely

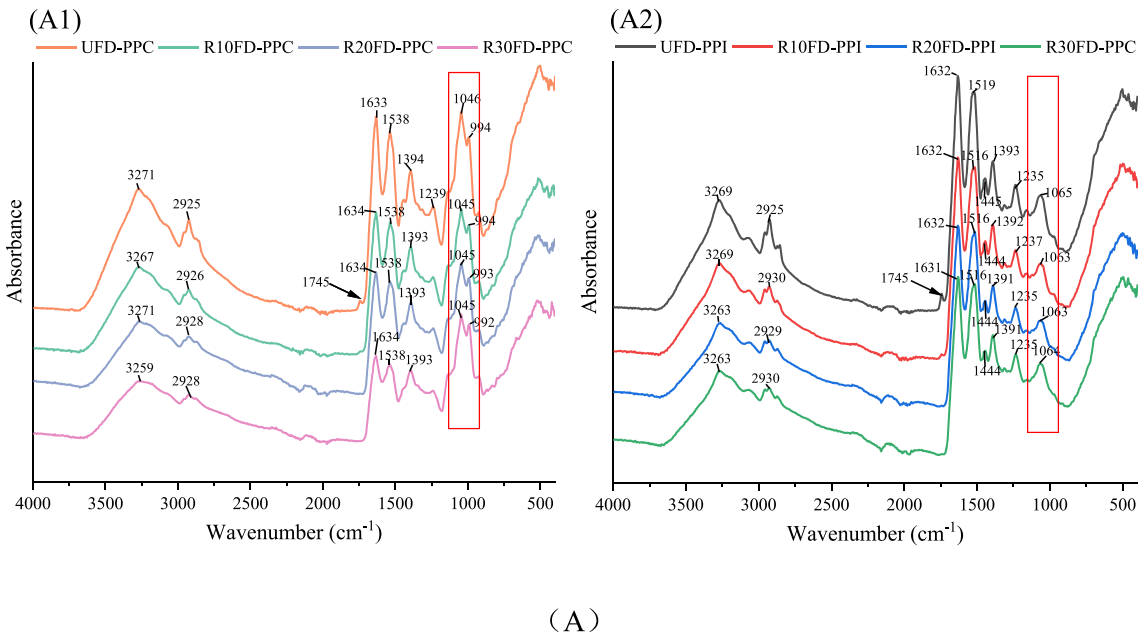

（A）

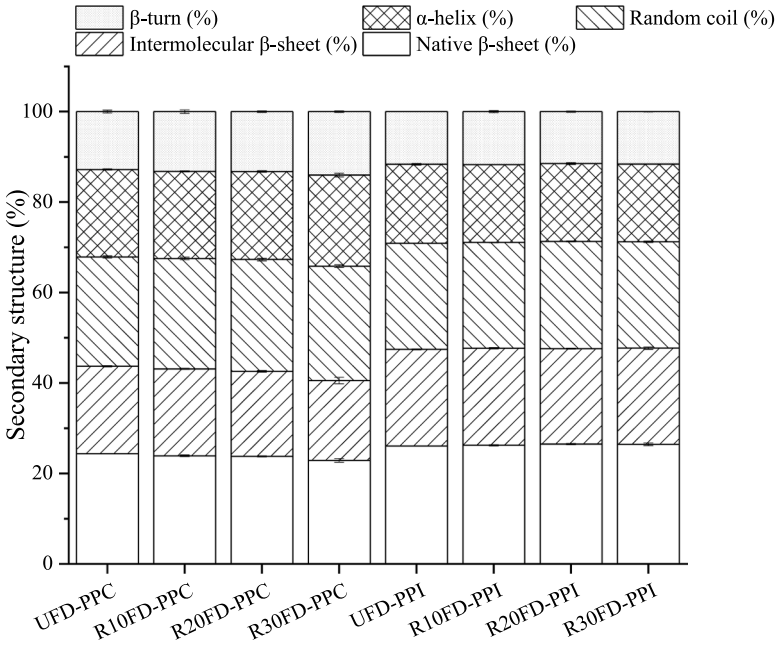

（B）

Fig. 4. **(A)** FT-IR spectra of **(A1)** PPC samples, and **(A2)** PPI samples. (The arrows show peaks at ~ 1745 cm^{-1} that have changed markedly, and the red frames mark the peaks between ~ 1100 and ~ 950 cm^{-1}). **(B)** Comparison of secondary structure content (%) in the amide I band of PPC and PPI with different pre-roasting times. (For interpretation of the references to colour in this figure legend, the reader is referred to the web version of this article.)

related to the unsaturated oxidation and beany flavour of yellow peas (Chang et al., 2022), and gradually vanished with the extension of roasting. The 66–71 kDa bands can be assigned to 7S convicilin or α-subunit of vicilin because of their high degree of homology (O'Kane et al., 2004). The strong bands with MW ranging from 53 to 57 kDa were denoted as legumin αβ at non-reducing condition (Fig. 3 **(A)**). Legumin αβ was cleaved into legumin α (~40 kDa) and legumin β (~20 kDa) bands due to the breakdown of interchain disulfide bonds under a reducing condition, resulting in the stronger bands in Fig. 3 **(B)** than that under non-reducing condition (Fig. 3 **(A)**), consistent with the studies reported by Chang et al. (2022) and Peng et al. (2016). The polypeptide fractions of vicilin were distributed at 46–50 kDa, 29–33 kDa, and < 15 kDa bands. The light bands with the lowest MW at ~ 10 kDa in the reducing electrophoretic image (Fig. 3 **(B)**) was probably ascribed to albumins (Rubio et al., 2014), which were only retained in PPC samples and absent in PPI samples. Interestingly, there was no band at ~ 10 kDa in the non-reducing image (Fig. 3 **(A)**), which may result from albumins with a high number of cysteine residues forming higher MW fractions with other albumin or non-albumin subunits through disulfide bonds (Higgins et al., 1986; Rubio et al., 2014). The lowest band intensity of the R30FD-PPC lane resulted from the lowest protein content (Table 1). Several broad stained bands above the protein bands (at high MW)

Table 2
Comparison of the content of total/free sulfhydryl (SH) and disulfide (SS) bonds in PPC and PPI with different pre-roasting times.

Samples	SH (μmol/g protein)		SS (μmol/g protein)
	Total	Free	
UFD-PPC	27.9 ± 0.5^{b}	25.4 ± 0.3^{a} ($91.1 \pm 1.9\%^{a}$)	1.2 ± 0.3^{f} ($4.5 \pm 1.0\%^{e}$)
R10FD-PPC	27.2 ± 0.6^{b}	20.0 ± 0.5^{b} ($73.6 \pm 0.6\%^{c}$)	3.6 ± 0.1^{d} ($13.2 \pm 0.3\%^{c}$)
R20FD-PPC	25.9 ± 0.5^{c}	13.1 ± 0.0^{e} ($50.7 \pm 1.1\%^{e}$)	6.4 ± 0.3^{a} ($24.6 \pm 0.5\%^{a}$)
R30FD-PPC	29.5 ± 0.5^{a}	17.1 ± 0.3^{d} ($57.9 \pm 1.6\%^{d}$)	6.2 ± 0.3^{a} ($21.1 \pm 0.8\%^{b}$)
UFD-PPI	22.2 ± 0.2^{d}	17.7 ± 0.2^{c} ($79.4 \pm 1.5\%^{b}$)	2.3 ± 0.2^{e} ($10.3 \pm 0.7\%^{d}$)
R10FD-PPI	20.4 ± 0.2^{e}	12.3 ± 0.1^{f} ($60.0 \pm 1.0\%^{d}$)	4.1 ± 0.1^{c} ($20.0 \pm 0.5\%^{b}$)
R20FD-PPI	19.0 ± 0.5^{f}	9.1 ± 0.1^{g} ($48.1 \pm 0.7\%^{e}$)	4.9 ± 0.2^{b} ($26.0 \pm 0.4\%^{a}$)
R30FD-PPI	19.5 ± 0.2^{f}	9.6 ± 0.5^{g} ($49.0 \pm 3.3\%^{e}$)	3.1 ± 0.1^{b} ($25.5 \pm 1.7\%^{a}$)

Different letters of the same column present significant differences ($P < 0.05$). The values in parentheses represent the percentage of free sulfhydryl and disulfide bonds, respectively.

became more visible with the longer roasting time, especially for samples that were roasted for 20 min and 30 min (lane 3, 4, 7 and 8), while there were no such bands in UFD-PPC/PPI. These observed staining areas in the high MW range could be attributed to the Maillard conjugates under roasting pre-treatment (Moscovici et al., 2014). The colour of these bands was darker in the RFD-PPI than in RFD-PPC samples since Coomassie bright blue only dyes proteins, which were much higher in PPI. In general, the electrophoretic profiles show pre-roasting induced the Maillard reaction but had a limited effect on the protein bands.

3.2.2. FT-IR analysis

FT-IR analysis is a common method to detect the changes in functional groups and secondary structures of proteins, which can track the conformational alteration of proteins under different treatment conditions. As found in Fig. 4 **(A)**, the broad asymmetric bands presented in the range of 3500–3000 cm^{-1} of all samples are predominantly associated with O–H stretching vibrations, indicating the presence of hydrogen bonds (Lin et al., 2021). The changes of O–H stretching band (both intensity and bandshape) in PPC and PPI were observed by normalising all the spectra using the intensity of the amide I band as a reference (**Fig. S1**). The spectral comparison shown in **Fig. S1 (A)** reveals not only that the intensities of the O–H stretching bands observed for PPC samples are significantly stronger, but also that the shapes of the O–H stretching bands are broader than those of PPI samples. Considering the presence of strong characteristic peaks associated with carbohydrates (1100-950 cm^{-1}) (Rodriguez-Huezo et al., 2022) in the normalised FTIR spectra of the PPC samples (**Fig. S1 (A)**), the higher intensities of the O–H stretching bands in the PPC samples were caused by an additional contribution of the –OH groups in the carbohydrates. This resulted in a more complex and higher level of intermolecular hydrogen bonding, which led to broader O–H stretching bands in the PPC samples. The PPI samples with much lower carbohydrate contents (Table 1) possess a lesser extent of intermolecular hydrogen bonding interaction, showing sharper O–H stretching bands.

It should be noted that the distinct peak at ~ 1745 cm^{-1} is assignable to ν(C = O) stretching mode of esters from lipid triglycerides and fatty acids, thereby it has been commonly used to represent total lipids in analysed samples (Guillen & Cabo, 1997). As shown in Fig. 4 **(A)**, although yellow split peas have a relatively low lipid content (2.7% wt), this peak was observed in both unroasted (control) PPC and PPI samples. However, the peak revealed a significant decrease in the intensity after 10 min of the pre-roasting process before totally disappearing in the samples that were pre-roasted for 20 min and longer. The disappearance of this peak suggests the potential oxidative cleavage of the lipid carbonyl band with long pre-roasting process (i.e., more than 10 min).

In addition, the amide I band (80% C=O stretching) in the range of 1700-1600 cm^{-1} is primarily used to assign secondary structures to proteins, which can estimate the fraction of β-sheet, β-turn, α-helix and random coil conformations to evaluate the protein aggregation and stability (Carbonaro & Nucara, 2010). As shown in Fig. 4 **(B)**, with the roasting time prolonging, β-sheet (including native and intermolecular structure) presented a decreasing trend in PPC, while the percentages of random coil and β-turn increased, especially for R30FD-PPC. The conversion from β-sheet to β-turn and random coil indicated that the secondary structure of PPC was more disordered after roasting due to high-temperature stress. Wang et al. (2017) suggested that high-temperature treatment enabled to decrease β-sheet and increase random coil/β-turn by impairing the hydrogen bonding of proteins secondary structures. Tatham et al. (1985) reported that β-turn requires fewer hydrogen bonds than the multiple bonded β-sheet structure due to its open reverse-turn structure. Therefore, from the secondary structure changes in PPC of the amide I band, it can be inferred that the hydrogen bonds of protein structures were partially damaged after pre-roasting treatment. The intermolecular β-sheet structure associated with protein aggregation was present in all PPC samples, and the percentage decreased with the extension of roasting treatment, but it was only significant ($P < 0.05$) in R30FD-PPC. This may be contrary to the common results that heating increased intermolecular β-sheet and induced protein aggregation (Murayama & Tomida, 2004), which could be because the heating subject in this study was pea seeds instead of the extracted proteins. As a result, compared to extracted proteins, protein bodies restricted within dried pea cells would not experience notable aggregation during heating (Kornet et al., 2020). In contrast, the secondary structure percentages of PPI with the prominently higher β-sheets and lower random coil, α-helix, and β-turn ($P < 0.05$) than PPC showed insignificant changes after roasting. The difference between the secondary structures of PPC and PPI is mainly because of their different extraction methods. PPC extracted from mild one-step alkaline dissolution contained more original structural proteins derived from pea seeds. PPI underwent harsher extraction conditions than PPC and isoelectric precipitation with extreme acid pH could lead to irreversible aggregation of pea globulins (Gueguen et al., 1988; Kornet et al., 2020) so that PPI contained more intermolecular (hydrogen-bonded) β-sheet (Fig. 4 **(B)**) contributing to aggregation (Shivu et al., 2013). In addition, the different protein types in extracted PPI (globulins) and PPC (globulins and albumins) could lead to the differences in their proportion of native β-sheet, random coil, α-helix, and β-turn (Kornet et al., 2020; Sosa et al., 2021). Overall, it can be speculated that in the amide I band, the extraction process played a major role in the percentage distribution of secondary structures in PPI, while pre-roasting enabled to influence the secondary structures of PPC.

The features of the amide II band (1550–1500 cm^{-1}, 60% N–H bending and 40% C–N stretching) interestingly revealed substantial differences between the PPC and PPI (Fig. 4 **(A)** and **S1** (B)). While the FT-IR spectra of all the PPC samples show the amide II band centred at ~ 1540 cm^{-1}, the spectra of the PPI samples indicate a significant red shift of the amide II band to ~ 1515 cm^{-1}, which were associated with the transformation of parallel β-sheet (1550-1530 cm^{-1}) to antiparallel β-sheet (1530-1510 cm^{-1}) protein structures due to isoelectric precipitation (Pelton & McLean, 2000). Moreover, PPI samples show an increase of intensity at ~ 1515 cm^{-1} (**Fig S1 (B)**), suggesting that the antiparallel β-sheet in the PPI samples is sensitive to the pre-roasting. Antiparallel β-sheet with well-oriented hydrogen bonds in the main

chain reportedly can withstand greater distortions and is more stable than parallel β-sheet structure (Kobayashi et al., 1995), suggesting that protein structures in PPI samples are likely to be more rigid than that in PPC due to different extraction process.

3.2.3. The content of sulfhydryl (SH) and disulfide (SS) bonds

The content of SH and SS can characterise the tertiary structure of proteins and reflect the protein conformation. As shown in Table 2, roasting greatly changed ($P < 0.05$) the total SH content of R20FD-PPC and R30FD-PPC, while it had little effect on the content of R10FD-PPC. All RFD-PPI samples showed a significant decrease ($P < 0.05$) in the total content of SH compared with UFD-PPI. Pre-roasting altered the solubility and shifted the isoelectric point of proteins in pea flour, which could be observed from the various yields of PPC or PPI under the same extraction process (Table 1). Similarly, the sulfur-containing amino acids content of obtained proteins could be various due to the change in properties of pea flours used for protein extraction. Apart from this observation, PPC contained more total sulfhydryl than the PPI counterparts (extracted from the same pea flour) since PPC samples contained higher thiol groups of albumins (Higgins et al., 1986; Rubio et al., 2014).

Using the percentage (in parentheses of Table 2) to describe the content of free SH and SS can eliminate the impact of different proteins with various total sulfhydryl content (Cui et al., 2020). Relatively short roasting times (10 and 20 min) could promote the oxidation of free SH groups to form SS bonds (Table 2). Delcour et al. (2012) also found that heating facilitated the oxidation of SH to SS in heat-induced gluten. The percentage of SS bonds in R30FD-PPC (21.1%) was significantly lower ($P < 0.05$) than that of R20FD-PPC (24.6%), while their free SH content showed the opposite trend, indicating further cleavage of SS bonds may occur when the roasting time was longer than 20 min at 150 °C.

3.2.4. Surface hydrophobicity of pea proteins

Roasting can partially denature proteins and expose buried hydrophobic groups, increasing surface hydrophobicity (H_o) value (Guldiken et al., 2022). As seen in Fig. 5, the H_o of PPC first increased and then decreased with the extension of roasting time, and R10FD-PPC had the highest H_o. By contrast, the H_o of PPI increased with a longer roasting time. The H_o of UFD-PPI was higher than that of UFD-PPC since isoelectric precipitation removed the hydrophilic albumin, only leaving the hydrophobic globulins, while albumins still existed in PPC samples (Stone et al., 2015). Additionally, the albumins in pea protein are thought to require less energy to unfold than globulins (Kornet et al., 2022), such that R10FD-PPC exposed more hydrophobic sites and acquired significantly higher H_o than R10FD-PPI (Fig. 5). With roasting times (20 and 30 min) extending, more thermal energy was provided to unfold the PPI, which increased the exposed hydrophobic groups (i.e. higher H_o in Fig. 5) and promoted the formation of disulfide bonds by adjacent free SH groups (Table 2). Gong et al. (2016) suggested that the more hydrophobic groups, the more SS bonds are likely to be produced. As for PPC, however, with longer roasting times (20 and 30 min), the formed local hydrophobic core may be masked by more Maillard complexes or caramelisation by-products since it contained more non-protein components (mainly carbohydrates) than PPI (Table 1). In general, pre-roasting enhanced the surface hydrophobicity of proteins, especially for PPI.

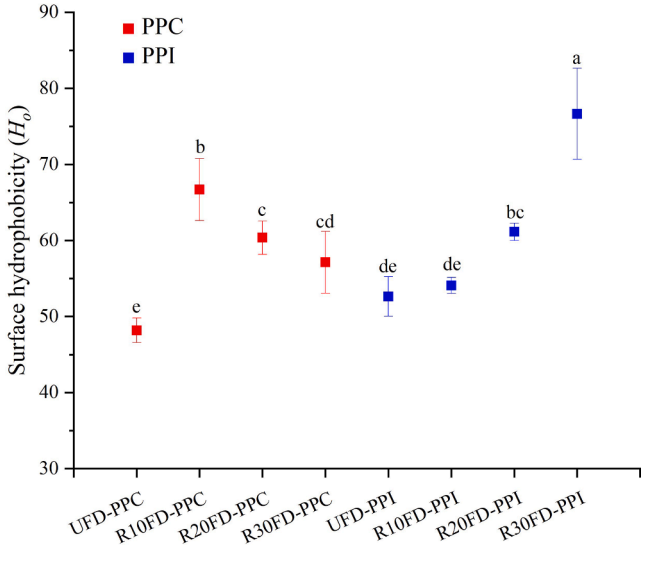

Fig. 5. Surface hydrophobicity of different pea protein extractions. Different letters show significant differences ($P < 0.05$).

3.3. Colour difference of the pea proteins

As shown in Table 3, among PPC and PPI samples, the L^* (lightness) values of proteins showed a decreasing trend with the increase of roasting time, especially the proteins extracted from pea seeds roasted for 30 min. By contrast, a^* (redness) values of proteins increased significantly ($P < 0.05$) with roasting pre-treatment for 20 min and 30 min. b^* (yellowness) values of RFD-PPC/PPI decreased significantly compared with unroasted pea proteins, while R20FD-PPC had the lowest yellowness values. The higher a^* may be due to the browning or caramel pigments produced by Maillard and caramelisation reactions during the roasting process (Ozdemir & Devres, 2000), while the reduction of b^* could result from the carotenoid oxidation-induced colour loss (Boon et al., 2010). Overall, after pre-roasting, protein powders became darker, redder, and less yellowish in colour (Fig. 6), and this trend of colour change was more pronounced in protein samples with longer roasting time (20 and 30 min).

3.4. Functional properties of proteins

3.4.1. EAI and ESI of protein samples

EAI estimates the surface area that can be stabilised per unit weight of protein by measuring the turbidity of the newly formed emulsion, reflecting the initial adsorption behaviour of proteins at the water–oil interface. ESI represents the capacity to impart strength to emulsions over a defined period and resist destabilising changes (Boye et al., 2010). From Fig. 7, the EAI of RFD-PPC or RFD-PPI showed an upward trend compared with unroasted samples. This may be because pre-roasting improved the solubility of the protein samples at pH 7 so that proteins had higher efficiency to form emulsions (Karaca et al., 2011). Except for a slight drop in R30FD-PPC, the EAI values of other PPC increased with longer roasting time, while the EAI of all PPI samples showed an increasing trend with longer roasting time, which may be due to the reduced mean particle sizes ($P < 0.05$) of RFD-PPC/PPI (Fig. 2 **(B)**). The small particle size of proteins could increase the migration rate and promote the adsorption at water/oil interface, lowering the interfacial tension (Liu et al., 2022). R20FD-PPC had the similar particle size

Table 3
L^*, a^*, b^* values of PPC and PPI with different pre-roasting times.

Samples	L^*	a^*	b^*
UFD-PPC	83.6 ± 0.3^{a}	2.2 ± 0.1^{f}	17.7 ± 0.3^{b}
R10FD-PPC	82.1 ± 0.7^{b}	1.8 ± 0.1^{g}	15.1 ± 0.1^{c}
R20FD-PPC	80.7 ± 0.6^{c}	3.2 ± 0.1^{e}	13.1 ± 0.5^{f}
R30FD-PPC	76.4 ± 0.3^{e}	4.9 ± 0.1^{c}	14.5 ± 0.2^{d}
UFD-PPI	80.9 ± 0.2^{c}	3.9 ± 0.0^{d}	19.8 ± 0.1^{a}
R10FD-PPI	80.3 ± 0.6^{cd}	3.8 ± 0.1^{d}	15.1 ± 0.2^{c}
R20FD-PPI	79.6 ± 0.9^{d}	5.5 ± 0.1^{b}	14.2 ± 0.4^{d}
R30FD-PPI	75.9 ± 0.5^{e}	6.6 ± 0.1^{a}	13.8 ± 0.2^{e}

Different letters in the same colourimetric values (L^*, a^*, b^*) show significant differences ($P < 0.05$).

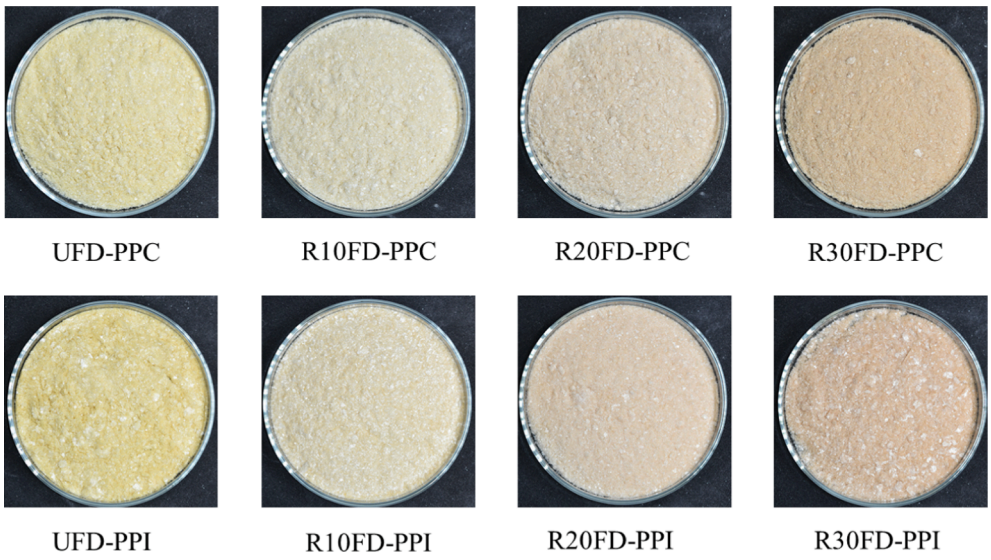

Fig. 6. Sample images of pea protein powders under different pre-roasting treatments.

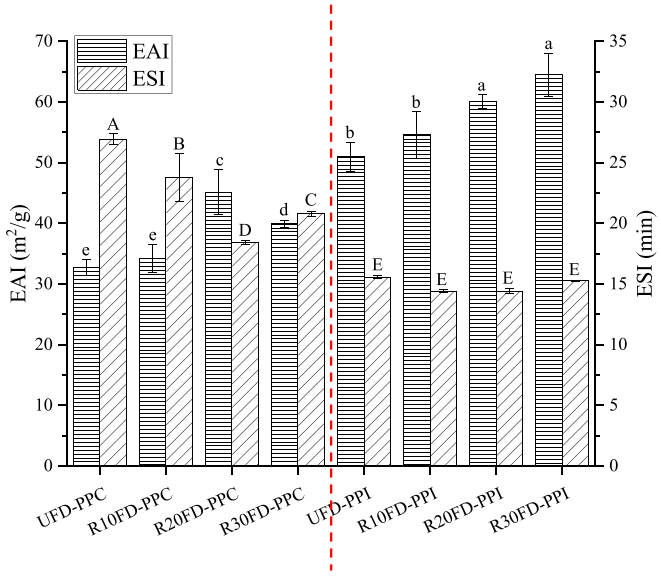

Fig. 7. Emulsion ability index (EAI) and Emulsion stability index (ESI) at pH 7 of different pea protein powders (The red dotted line separates the PPC and PPI samples). Different letters of the same category mean significant differences ($P < 0.05$). (For interpretation of the references to colour in this figure legend, the reader is referred to the web version of this article.)

to R30FD-PPC, whereas it showed significantly higher EAI ($P < 0.05$), which possibly because R20FD-PPC contained much higher proteins (Table 1) and had the same protein solubility as R30FD-PPC at pH 7 (Fig. 2 **(A1)**). As a result, the water–oil surface in R20FD-PPC based emulsion was stabilised by more soluble proteins than that in R30FD-PPC so that the higher EAI of R20FD-PPC was obtained. Surprisingly, albumin-containing PPC had significantly lower EAI values ($P < 0.05$) than the PPI (Fig. 7), though albumins with smaller molecule weight and lower surface adsorption energy could diffuse faster to the water–oil interface than bigger globulins (Kornet et al., 2021b). According to the surface pressure test conducted by Kornet et al. (2022), globulins dominated the emulsifying properties of PPC, and it can be speculated that globulins have better amphiphilicity than albumins and are easier to be adsorbed in the water–oil interface. Thus, PPC with fewer globulins exhibited lower EAI.

However, the ESI of RFD-PPC was significantly lower than that of UFD-PPC, which was opposite to the trend of EAI. Due to the impurity of PPC, the resulting Maillard or caramelisation products in RFD-PPC could decrease the surface charge of proteins, leading to a lower steric repulsion between the oil droplets so that they are more likely to induce collision and flocculation of droplets (Zhao et al., 2022). ESI of PPI did not change much before and after roasting, possibly because of its higher purity with less non-protein components interference. It is worth noting that PPC presented higher ESI than PPI, which may be because albumins and globulins contained in PPC could synergistically match and adsorb on the water–oil interface to stabilise the emulsion better. More specifically, albumins are smaller and have a lower net protein charge than globulins (Yang et al., 2022b), which allows albumins to fit more easily on the interface and approach closely with low electrostatic repulsion (Kornet et al., 2021b). Overall, pre-roasting can promote EAI of both PPC and PPI samples, while it decreased the ESI of PPC and had no significant effect on the ESI of PPI.

3.4.2. *Thermal properties*

Thermal properties showed the thermal stability or denaturation degree of proteins. Fig. 8 **(A)** displays the representative heat flow patterns of PPC and PPI, showing that all samples had endothermic peaks between 80 and 100 °C. Thus, the roasting conditions (roasted at 150 °C for 10, 20, and 30 min) in this study did not cause complete denaturation of pea proteins. Fig. 8 **(B)** shows the onset temperature (T_o) and denaturation temperature (T_d) that were required for the denaturation of each protein powder. The ΔH of all pea proteins tend to decrease after roasting, but there was no significant difference among all samples (Fig. 8 **(C)**), further proving that the pre-roasting in this study only partially denatured the pea proteins.

The T_o of PPC did not change much, while their T_d first decreased and then increased with the roasting time extending. The reduction of T_d in R10FD-PPC and R20FD-PPC, presenting their thermal stability was impaired, though the average temperature of decrease was only within 5 °C (from 93.7 ± 2.0 to 89.0 ± 3.2 °C), which may be caused by the decreasing of rigid β-sheets (Fig. 4 **(B)**) of PPC. Surprisingly, the T_d of the R30FD-PPC was increased, which could be due to its prominent low protein content and high carbohydrates (Table 1), and most carbohydrates are soluble oligosaccharides and polysaccharides (Kornet et al., 2020). As a result, more soluble carbohydrates containing hydroxyl groups formed non-specifically extensive hydrogen bonds around the hydration shell of protein, thereby improving the overall T_d of R30FD-PPC (Kaushik & Bhat, 1998). The T_d of PPI showed no significant

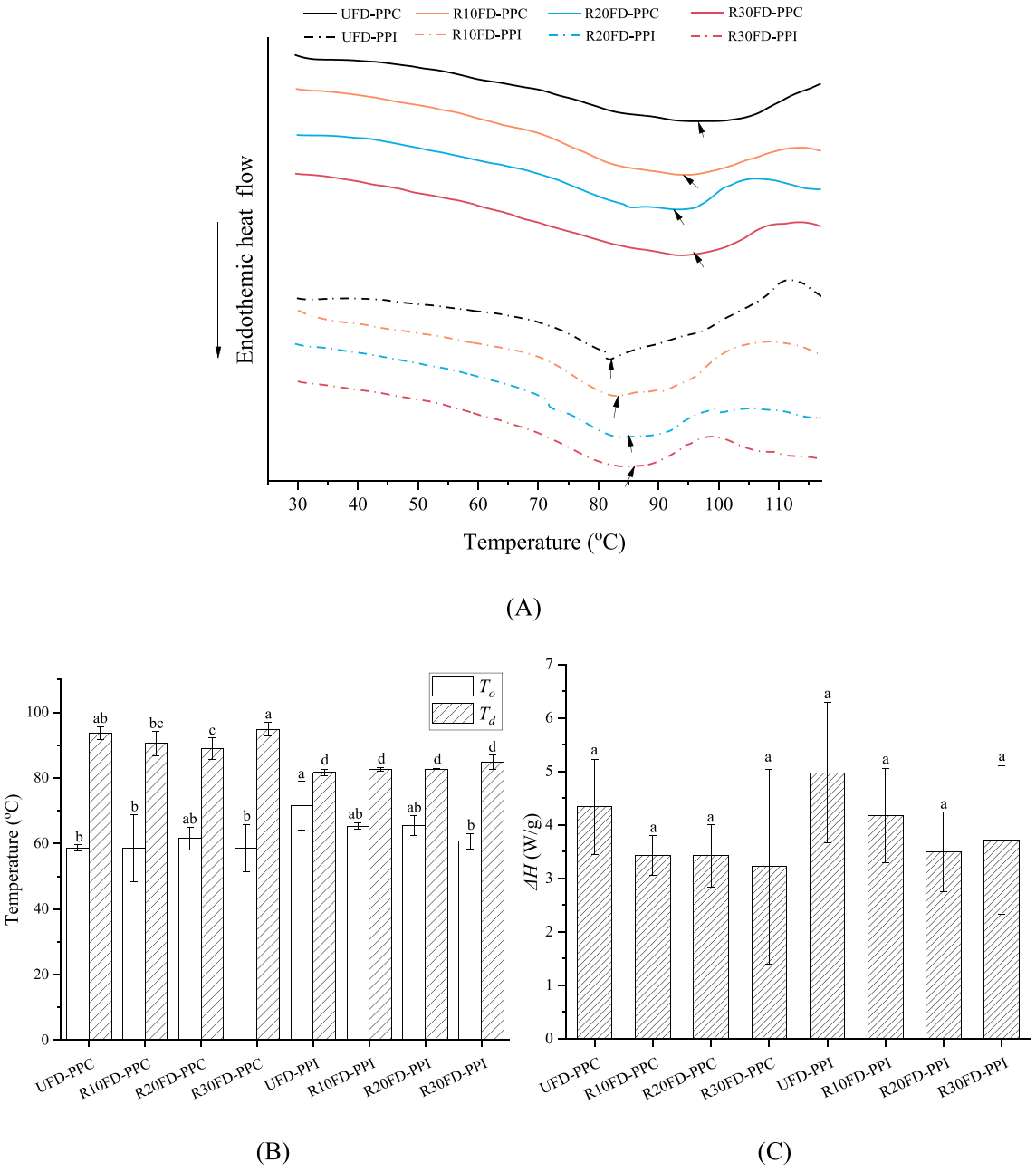

Fig. 8. **(A)** DSC thermographs of pea protein powders (The arrows in the figure show the lowest point of the peaks). Comparison of the **(B)** onset temperature (T_o), denaturation temperature (T_d), and (C) enthalpy (ΔH) of different pea proteins. Different letters in the same parameter mean significant differences ($P < 0.05$).

changes, which could be explained by the conformation of PPI samples with more rigid β-sheet while referring to their secondary structural analysis (Fig. 4 **(B)**) so that their T_d was almost unaffected by pre-roasting treatment. Despite this, the T_o of PPI decreased prominently with the extension of roasting time, indicating the RFD-PPI was partially denatured by pre-roasting and only a lower temperature was required to trigger initial denaturation than that of UFD-PPI. The significant changes in the tertiary structures (Table 2 **and** Fig. 6) of PPI samples also suggested that their native conformation was altered.

Compared to the T_o and T_d of PPC and PPI extracted from the same pea flour, PPC had higher T_d but lower T_o than the corresponding PPI samples. PPC contains more starch residues than PPI (Table 1) since it omitted the process of isoelectric precipitation, which may cause the endothermic slope of PPC to appear near the temperature at which starch began to gelatinize (~59 °C) (Kornet et al., 2020; Kornet et al., 2021b). Additionally, PPI could remove most of the salt ions in basic pea protein extracts through the isoelectric precipitation, but PPC retains more ions like K^+ and P^{3+}, which possibly originate from phytic acid and K-phytate (Kornet et al., 2021c). The increasing T_d of PPC might be due to the presence of more endogenous salt ions, which could affect the electrostatic response, increase intramolecular hydrophobic associations and strengthen the hydration of protein suspension to increase the thermal stability (Shand et al., 2007). The more prominent intermolecular hydrogen bonds between proteins and carbohydrates of PPC samples detected in normalised FT-IR spectra (**Fig. S1 (A)**) can also be a reason for the higher T_d of PPC than PPI. To conclude, pre-roasting partially denatured the proteins, and T_d of PPC samples with shorter roasting time (R10FD-PPC and R20FD-PPC) and the T_o of RFD-PPI were slightly reduced.

4. Conclusion

Although all the roasting conditions increased the protein solubility around pH 7, short-term roasting (150 °C for 10 and 20 min) was beneficial as they did not compromise extraction efficiency. The solubility of RFD-PPI was much improved at pH 3, which could open its applications in acidic protein beverages. The SDS-PAGE profiles of PPC and PPI were almost unchanged under all roasting conditions, except for the broad stained bands presented in the top of gels with pre-roasting treatment, indicating the existence of high molecular weight Maillard conjugates. Moreover, as detected in the amide I band, roasting induced the decrease in native and intermolecular β-sheets and the increase in the random coil and β-turn in PPC, while only having a subtle impact on PPI. Nevertheless, the total/free SH, SS bond and *Ho* were significantly altered with longer roasting time. The changes in functional properties of pea proteins including solubility, emulsifying, and thermal properties were correlated to the effects of roasting times on conformation, extraction process (with or without isoelectric precipitation), and non-protein content (carbohydrates, etc.) of the protein powders. Considering the extraction efficiency and functionality of pea proteins, the pre-roasting at 150 °C for 10 or 20 min could be a promising pre-treatment method for the preparation of high-quality PPC and PPI. The outcomes provided a strategy for improving the solubility of pea proteins, while retaining their emulsifying and thermal properties. The strategy could be beneficial in the processing of pea proteins as ingredients for plant-based beverage production.

CRediT authorship contribution statement

Yanyan Lao: Methodology, Investigation, Formal analysis, Writing – original draft. **Qianyu Ye:** Methodology, Validation, Writing – review & editing. **Yong Wang:** Supervision, Writing – review & editing. **Jitraporn Vongsvivut:** Formal analysis, Writing – review & editing. **Cordelia Selomulya:** Supervision, Writing – review & editing, Project administration, Funding acquisition.

Declaration of Competing Interest

The authors declare that they have no known competing financial interests or personal relationships that could have appeared to influence the work reported in this paper.

Data availability

Data will be made available on request.

Acknowledgements

This project was supported by ARC Discovery grant (DP200100642). The authors would like to acknowledge the XRF Laboratory, Mark Wainwright Analytical Centre. We thank Dr. Nicholas Bedford and A/Prof Alice Lee for access to Malvern Zetasizer Nano, and the Bio-Rad Gel Dox XR system.

Appendix A. Supplementary material

Supplementary data to this article can be found online at https://doi.org/10.1016/j.foodres.2023.113180.

References

Boon, C. S., McClements, D. J., Weiss, J., & Decker, E. A. (2010). Factors influencing the chemical stability of carotenoids in foods. *Critical Reviews in Food Science and Nutrition, 50*(6), 515–532. https://doi.org/10.1080/10408390802565889

Boukid, F., Rosell, C. M., & Castellari, M. (2021). Pea protein ingredients: A mainstream ingredient to (re)formulate innovative foods and beverages. *Trends in Food Science & Technology, 110*, 729–742. https://doi.org/10.1016/j.tifs.2021.02.040

Boye, J. I., Aksay, S., Roufik, S., Ribereau, S., Mondor, M., Farnworth, E., & Rajamohamed, S. H. (2010). Comparison of the functional properties of pea, chickpea and lentil protein concentrates processed using ultrafiltration and isoelectric precipitation techniques. *Food Research International, 43*(2), 537–546. https://doi.org/10.1016/j.foodres.2009.07.021

Bradford, M. M. (1976). A rapid and sensitive method for the quantitation of microgram quantities of protein utilizing the principle of protein-dye binding. *Analytical Biochemistry, 72*, 248–254. https://doi.org/10.1006/abio.1976.9999

Burger, T. G., Singh, I., Mayfield, C., Baumert, J. L., & Zhang, Y. (2022). The impact of spray drying conditions on the physicochemical and emulsification properties of pea protein isolate. *Lwt-Food Science and Technology, 153*, Article 112495. https://doi.org/10.1016/j.lwt.2021.112495

Carbonaro, M., Maselli, P., & Nucara, A. (2012). Relationship between digestibility and secondary structure of raw and thermally treated legume proteins: A Fourier transform infrared (FT-IR) spectroscopic study. *Amino Acids, 43*(2), 911–921. https://doi.org/10.1007/s00726-011-1151-4

Carbonaro, M., & Nucara, A. (2010). Secondary structure of food proteins by Fourier transform spectroscopy in the mid-infrared region. *Amino Acids, 38*(3), 679–690. https://doi.org/10.1007/s00726-009-0274-3

Chang, L. Y., Lan, Y., Bandillo, N., Ohm, J. B., Chen, B. C., & Rao, J. J. (2022). Plant proteins from green pea and chickpea: Extraction, fractionation, structural characterization and functional properties. *Food Hydrocolloids, 123*, Article 107165. https://doi.org/10.1016/j.foodhyd.2021.107165

Cui, L. Q., Bandillo, N., Wang, Y. C., Ohm, J. B., Chen, B. C., & Rao, J. J. (2020). Functionality and structure of yellow pea protein isolate as affected by cultivars and extraction pH. *Food Hydrocolloids, 108*, Article 106008. https://doi.org/10.1016/j.foodhyd.2020.106008

Delcour, J. A., Joye, I. J., Pareyt, B., Wilderjans, E., Brijs, K., & Lagrain, B. (2012). Wheat gluten functionality as a quality determinant in cereal-based food products. *Annual Review of Food Science and Technology, 3*(1), 469–492. https://doi.org/10.1146/annurev-food-022811-101303

Doan, C. D., & Ghosh, S. (2019). Formation and stability of pea proteins nanoparticles using ethanol-induced desolvation. *Nanomaterials, 9*(7), 1–15. https://doi.org/10.3390/nano9070949

Fang, L. Y., Xiang, H., Sun-Waterhouse, D., Cui, C., & Lin, J. J. (2020). Enhancing the usability of pea protein isolate in food applications through modifying its structural and sensory properties via deamidation by glutaminase. *Journal of Agricultural and Food Chemistry, 68*(6), 1691–1697. https://doi.org/10.1021/acs.jafc.9b06046

Gao, K., Zha, F. C., Yang, Z. Y., Rao, J. J., & Chen, B. C. (2022). Structure characteristics and functionality of water-soluble fraction from high-intensity ultrasound treated pea protein isolate. *Food Hydrocolloids, 125*, Article 107409. https://doi.org/10.1016/j.foodhyd.2021.107409

Gao, Z. L., Shen, P. Y., Lan, Y., Cui, L. Q., Ohm, J. B., Chen, B. C., & Rao, J. J. (2020). Effect of alkaline extraction pH on structure properties, solubility, and beany flavor of yellow pea protein isolate. *Food Research International, 131*, Article 109045. https://doi.org/10.1016/j.foodres.2020.109045

Gong, K. J., Shi, A. M., Liu, H. Z., Liu, L., Hu, H., Adhikari, B., & Wang, Q. (2016). Emulsifying properties and structure changes of spray and freeze-dried peanut protein isolate. *Journal of Food Engineering, 170*, 33–40. https://doi.org/10.1016/j.jfoodeng.2015.09.011

Gorissen, S. H. M., Crombag, J. J. R., Senden, J. M. G., Waterval, W. A. H., Bierau, J., Verdijk, L. B., & van Loon, L. J. C. (2018). Protein content and amino acid composition of commercially available plant-based protein isolates. *Amino Acids, 50*(12), 1685–1695. https://doi.org/10.1007/s00726-018-2640-5

Gueguen, J., Chevalier, M., Barbot, J., & Schaeffer, F. (1988). Dissociation and aggregation of pea legumin induced by pH and ionic-strength. *Journal of the Science of Food and Agriculture, 44*(2), 167–182. https://doi.org/10.1002/jsfa.2740440208

Guillen, M. D., & Cabo, N. (1997). Infrared spectroscopy in the study of edible oils and fats. *Journal of the Science of Food and Agriculture, 75*(1), 1–11. https://doi.org/10.1002/(Sici)1097-0010(199709)75:1<1::Aid-Jsfa842>3.0.Co;2-R

Guldiken, B., Konieczny, D., Franczyk, A., Satiro, V., Pickard, M., Wang, N., … Nickerson, M. T. (2022). Impacts of infrared heating and tempering on the chemical composition, morphological, functional properties of navy bean and chickpea flours. *European Food Research and Technology, 248*(3), 767–781. https://doi.org/10.1007/s00217-021-03918-4

Higgins, T. J. V., Chandler, P. M., Randall, P. J., Spencer, D., Beach, L. R., Blagrove, R. J., … Inglis, A. S. (1986). Gene structure, protein structure, and regulation of the synthesis of a sulfur-rich protein in pea seeds. *Journal of Biological Chemistry, 261*(24), 1124–1130. https://doi.org/10.1016/s0021-9258(18)67357-0

Jiang, S. S., Ding, J. Z., Andrade, J., Rababah, T. M., Almajwal, A., Abulmeaty, M. M., & Feng, H. (2017). Modifying the physicochemical properties of pea protein by pH-shifting and ultrasound combined treatments. *Ultrasonics Sonochemistry, 38*, 835–842. https://doi.org/10.1016/j.ultsonch.2017.03.046

Karaca, A. C., Low, N., & Nickerson, M. (2011). Emulsifying properties of chickpea, faba bean, lentil and pea proteins produced by isoelectric precipitation and salt extraction. *Food Research International, 44*(9), 2742–2750. https://doi.org/10.1016/j.foodres.2011.06.012

Kaushik, J. K., & Bhat, R. (1998). Thermal stability of proteins in aqueous polyol solutions: Role of the surface tension of water in the stabilizing effect of polyols. *Journal of Physical Chemistry B, 102*(36), 7058–7066. https://doi.org/10.1021/jp981119l

Kent, R. M., & Doherty, S. B. (2014). Probiotic bacteria in infant formula and follow-up formula: Microencapsulation using milk and pea proteins to improve microbiological quality. *Food Research International, 64*, 567–576. https://doi.org/10.1016/j.foodres.2014.07.029

Kim, W., Wang, Y., & Selomulya, C. (2022). Impact of sodium alginate on binary whey/pea protein-stabilised emulsions. *Journal of Food Engineering, 321*, Article 110978. https://doi.org/10.1016/j.jfoodeng.2022.110978

Kobayashi, K., Granja, J. R., & Ghadiri, M. R. (1995). β-Sheet peptide architecture: Measuring the relative stability of parallel vs. antiparallel β-sheets. *Angewandte Chemie International Edition in English, 34*(1), 95–98. 10.1002/anie.199500951.

Kong, J., & Yu, S. (2007). Fourier transform infrared spectroscopic analysis of protein secondary structures. *Acta Biochimica Et Biophysica Sinica, 39*(8), 549–559. https://doi.org/10.1111/j.1745-7270.2007.00320.x

Kornet, C., Venema, P., Nijsse, J., van der Linden, E., van der Goot, A. J., & Meinders, M. (2020). Yellow pea aqueous fractionation increases the specific volume fraction and viscosity of its dispersions. *Food Hydrocolloids, 99*, Article 105332. https://doi.org/10.1016/j.foodhyd.2019.105332

Kornet, R., Penris, S., Venema, P., van der Goot, A. J., Meinders, M. B. J., & van der Linden, E. (2021c). How pea fractions with different protein composition and purity can substitute WPI in heat-set gels. *Food Hydrocolloids, 120*, Article 106891. https://doi.org/10.1016/j.foodhyd.2021.106891

Kornet, R., Shek, C., Venema, P., van der Goot, A. J., Meinders, M., & van der Linden, E. (2021a). Substitution of whey protein by pea protein is facilitated by specific fractionation routes. *Food Hydrocolloids, 117*, Article 106691. https://doi.org/10.1016/j.foodhyd.2021.106691

Kornet, R., Veenemans, J., Venema, P., van der Goot, A. J., Meinders, M., Sagis, L., & van der Linden, E. (2021b). Less is more: Limited fractionation yields stronger gels for pea proteins. *Food Hydrocolloids, 112*, Article 106285. https://doi.org/10.1016/j.foodhyd.2020.106285

Kornet, R., Yang, J., Venema, P., van der Linden, E., & Sagis, L. M. C. (2022). Optimizing pea protein fractionation to yield protein fractions with a high foaming and emulsifying capacity. *Food Hydrocolloids, 126*, Article 107456. https://doi.org/10.1016/j.foodhyd.2021.107456

Kutzli, I., Griener, D., Gibis, M., Schmid, C., Dawid, C., Baier, S. K., … Weiss, J. (2020). Influence of Maillard reaction conditions on the formation and solubility of pea protein isolate-maltodextrin conjugates in electrospun fibers. *Food Hydrocolloids, 101*, Article 105535. https://doi.org/10.1016/j.foodhyd.2019.105535

Lin, H., Bean, S. R., Tilley, M., Peiris, K. H. S., & Brabec, D. (2021). Qualitative and quantitative analysis of sorghum grain composition including protein and tannins using ATR-FTIR spectroscopy. *Food Analytical Methods, 14*(2), 268–279. https://doi.org/10.1007/s12161-020-01874-5

Liu, X., Wang, M., Xue, F., & Adhikari, B. (2022). Application of ultrasound treatment to improve the technofunctional properties of hemp protein isolate. *Future Foods, 6*, Article 100176. 10.1016/j.fufo.2022.100176.

Ma, Z., Boye, J. I., Simpson, B. K., Prasher, S. O., Monpetit, D., & Malcolmson, L. (2011). Thermal processing effects on the functional properties and microstructure of lentil, chickpea, and pea flours. *Food Research International, 44*(8), 2534–2544. https://doi.org/10.1016/j.foodres.2010.12.017

Markets. (2022). *Plant-based Protein Market-Global Forecast to 2027*. https://www.marketsandmarkets.com/Market-Reports/plant-based-protein-market-14715651.html.

Masuko, T., Minami, A., Iwasaki, N., Majima, T., Nishimura, S. I., & Lee, Y. C. (2005). Carbohydrate analysis by a phenol-sulfuric acid method in microplate format. *Analytical Biochemistry, 339*(1), 69–72. https://doi.org/10.1016/j.ab.2004.12.001

Meng, G. T., & Ma, C. Y. (2001). Fourier-transform infrared spectroscopic study of globulin from Phaseolus angularis (red bean). *International Journal of Biological Macromolecules, 29*(4–5), 287–294. https://doi.org/10.1016/S0141-8130(01)00178-7

Mesfin, N., Belay, A., & Amare, E. (2021). Effect of germination, roasting, and variety on physicochemical, techno-functional, and antioxidant properties of chickpea (Cicer arietinum L.) protein isolate powder. *Heliyon, 7*(9), 1-8. https://doi.org/10.1016/j.heliyon.2021.e08081.

Mession, J. L., Sok, N., Assifaoui, A., & Saurel, R. (2013). Thermal denaturation of pea globulins (*Pisum sativum L.*) - Molecular interactions leading to heat-induced protein aggregation. *Journal of Agricultural and Food Chemistry, 61*(6), 1196–1204. https://doi.org/10.1021/jf303739n

Moscovici, A. M., Joubran, Y., Briard-Bion, V., Mackie, A., Dupont, D., & Lesmes, U. (2014). The impact of the Maillard reaction on the in vitro proteolytic breakdown of bovine lactoferrin in adults and infants. *Food & Function, 5*(8), 1898–1908. https://doi.org/10.1039/c4fo00248b

Murayama, K., & Tomida, M. (2004). Heat-induced secondary structure and conformation change of bovine serum albumin investigated by Fourier transform infrared spectroscopy. *Biochemistry, 43*(36), 11526–11532. https://doi.org/10.1021/bi0489154

Nagai, R., Ikeda, K., Kawasaki, Y., Sano, H., Yoshida, M., Araki, T., … Horiuchi, S. (1998). Conversion of Amadori product of Maillard reaction to Nε-(carboxymethyl) lysine in alkaline condition. *FEBS Letters, 425*(2), 355–360. 10.1016/S0014-5793(98)00263-4.

Neucere, N. J. (1972). Effect of heat on peanut proteins. I. Solubility properties and immunochemical-electrophoretic modifications. *Journal of Agricultural and Food Chemistry, 20*(2), 252–255. https://doi.org/10.1021/jf60180a030

O'Kane, F. E., Happe, R. P., Vereijken, J. M., Gruppen, H., & van Boekel, M. A. J. S. (2004). Characterization of pea vicilin. 1. Denoting convicilin as the alpha-subunit of the Pisum vicilin family. *Journal of Agricultural and Food Chemistry, 52*(10), 3141–3148. https://doi.org/10.1021/jf035104i

Ozdemir, M., & Devres, O. (2000). Kinetics of color changes of hazelnuts during roasting. *Journal of Food Engineering, 44*(1), 31–38. https://doi.org/10.1016/S0260-8774(99)00162-4

Pelton, J. T., & McLean, L. R. (2000). Spectroscopic methods for analysis of protein secondary structure. *Analytical Biochemistry, 277*(2), 167–176. https://doi.org/10.1006/abio.1999.4320

Peng, W. W., Kong, X. Z., Chen, Y. M., Zhang, C. M., Yang, Y. X., & Hua, Y. F. (2016). Effects of heat treatment on the emulsifying properties of pea proteins. *Food Hydrocolloids, 52*, 301–310. https://doi.org/10.1016/j.foodhyd.2015.06.025

Rodriguez-Huezo, M. E., Valeriano-Garcia, N., Totosaus-Sanchez, A., Vernon-Carter, E. J., & Alvarez-Ramirez, J. (2022). The effect of the addition of soluble fibers (polydextrose, corn, pea) on the color, texture, structural features and protein digestibility of semolina pasta. *Applied Food Research, 2*(2), Article 100187. 10.1016/j.afres.2022.100187.

Rubio, L. A., Perez, A., Ruiz, R., Guzman, M. A., Aranda-Olmedo, I., & Clemente, A. (2014). Characterization of pea (*Pisum sativum*) seed protein fractions. *Journal of the Science of Food and Agriculture, 94*(2), 280–287. https://doi.org/10.1002/jsfa.6250

Shand, P. J., Ya, H., Pietrasik, Z., & Wanasundara, P. K. J. P. D. (2007). Physicochemical and textural properties of heat-induced pea protein isolate gels. *Food Chemistry, 102*(4), 1119–1130. https://doi.org/10.1016/j.foodchem.2006.06.060

Sharif, H. R., Williams, P. A., Sharif, M. K., Abbas, S., Majeed, H., Masamba, K. G., … Zhong, F. (2018). Current progress in the utilization of native and modified legume proteins as emulsifiers and encapsulants - A review. *Food Hydrocolloids, 76*, 2–16. https://doi.org/10.1016/j.foodhyd.2017.01.002

Shen, Y. T., Hong, S., Singh, G., Koppel, K., & Li, Y. H. (2022). Improving functional properties of pea protein through "green" modifications using enzymes and polysaccharides. *Food Chemistry, 385*, Article 132687. https://doi.org/10.1016/j.foodchem.2022.132687

Shen, Y. T., Tang, X., & Li, Y. H. (2021). Drying methods affect physicochemical and functional properties of quinoa protein isolate. *Food Chemistry, 339*, Article 127823. https://doi.org/10.1016/j.foodchem.2020.127823

Shivu, B., Seshadri, S., Li, J., Oberg, K. A., Uversky, V. N., & Fink, A. L. (2013). Distinct β-sheet structure in protein aggregates determined by ATR–FTIR spectroscopy. *Biochemistry, 52*(31), 5176–5183. https://doi.org/10.1021/bi400625v

Skylas, D. J., Molloy, M. P., Willows, R. D., Blanchard, C. L., & Quail, K. J. (2017). Characterisation of protein isolates prepared from processed mungbean (*Vigna radiata*) flours. *Journal of Agricultural Science, 9*(12), 1–10. https://doi.org/10.5539/jas.v9n12p1

Sosa, E. I. F., Chaves, M. G., Quiroga, A. V., & Avanza, M. V. (2021). Comparative study of structural and physicochemical properties of pigeon pea (*Cajanus cajan L.*) protein isolates and its major protein fractions. *Plant Foods for Human Nutrition, 76*(1), 37–45. https://doi.org/10.1007/s11130-020-00871-7

Sridharan, S., Meinders, M. B. J., Bitter, J. H., & Nikiforidis, C. V. (2020). On the emulsifying properties of self-assembled pea protein particles. *Langmuir, 36*(41), 12221–12229. https://doi.org/10.1021/acs.langmuir.0c01955

Stone, A. K., Karalash, A., Tyler, R. T., Warkentin, T. D., & Nickerson, M. T. (2015). Functional attributes of pea protein isolates prepared using different extraction methods and cultivars. *Food Research International, 76*, 31–38. https://doi.org/10.1016/j.foodres.2014.11.017

Stone, A. K., Parolia, S., House, J. D., Wang, N., & Nickerson, M. T. (2021). Effect of roasting pulse seeds at different tempering moisture on the flour functional properties and nutritional quality. *Food Research International, 147*, Article 110489. https://doi.org/10.1016/j.foodres.2021.110489

Tanger, C., Engel, J., & Kulozik, U. (2020). Influence of extraction conditions on the conformational alteration of pea protein extracted from pea flour. *Food Hydrocolloids, 107*, Article 105949. https://doi.org/10.1016/j.foodhyd.2020.105949

Tatham, A. S., Miflin, B. J., & Shewry, P. R. (1985). The beta-turn conformation in wheat gluten proteins: Relationship to gluten elasticity. *Cereal Chemistry, 62*(5), 405–412. <Go to ISI>://WOS:A1985ASS4500017.

Tenorio, A. T., Kyriakopoulou, K. E., Suarez-Garcia, E., van den Berg, C., & van der Goot, A. J. (2018). Understanding differences in protein fractionation from conventional crops, and herbaceous and aquatic biomass - Consequences for industrial use. *Trends in Food Science & Technology, 71*, 235–245. https://doi.org/10.1016/j.tifs.2017.11.010

Vallath, A., Shanmugam, A., & Rawson, A. (2022). Prospects of future pulse milk variants from other healthier pulses-As an alternative to soy milk. *Trends in Food Science & Technology, 124*, 51–62. https://doi.org/10.1016/j.tifs.2022.03.028

Wang, Y., Chen, Y. H., Zhou, Y., Nirasawa, S., Tatsumi, E., Li, X. T., & Cheng, Y. Q. (2017). Effects of konjac glucomannan on heat-induced changes of wheat gluten structure. *Food Chemistry, 229*, 409–416. https://doi.org/10.1016/j.foodchem.2017.02.056

Yang, J., Kornet, R., Diedericks, C. F., Yang, Q. H. Z., Berton-Carabin, C. C., Nikiforidis, C. V., … Sagis, L. M. C. (2022b). Rethinking plant protein extraction: Albumin-from side stream to an excellent foaming ingredient. *Food Structure, 31*, Article 100254. https://doi.org/10.1016/j.foostr.2022.100254

Yang, J., Mocking-Bode, H. C. M., van den Hoek, I. A. F., Theunissen, M., Voudouris, P., Meinders, M. B. J., & Sagis, L. M. C. (2022a). The impact of heating and freeze or spray drying on the interface and foam stabilising properties of pea protein extracts: Explained by aggregation and protein composition. *Food Hydrocolloids, 133*, Article 107913. https://doi.org/10.1016/j.foodhyd.2022.107913

Yang, S. N., Li, X. F., Hua, Y. F., Chen, Y. M., Kong, X. Z., & Zhang, C. M. (2020). Selective complex coacervation of pea whey proteins with chitosan to purify main 2S albumins. *Journal of Agricultural and Food Chemistry, 68*(6), 1698–1706. https://doi.org/10.1021/acs.jafc.9b06311

Yu, H., Zhang, R. Y., Yang, F. W., Xie, Y. F., Guo, Y. H., Yao, W. R., & Zhou, W. B. A. (2021). Control strategies of pyrazines generation from Maillard reaction. *Trends in Food Science & Technology, 112*, 795–807. https://doi.org/10.1016/j.tifs.2021.04.028

Zaaboul, F., Raza, H., Chen, C., & Liu, Y. F. (2019). The impact of roasting, high pressure homogenization and sterilization on peanut milk and its oil bodies. *Food Chemistry, 280*, 270–277. https://doi.org/10.1016/j.foodchem.2018.12.047

Zandomeneghi, G., Krebs, M. R., McCammon, M. G., & Fändrich, M. (2004). FTIR reveals structural differences between native β-sheet proteins and amyloid fibrils. *Protein science, 13*(12), 3314–3321. https://doi.org/10.1110/ps.041024904

Zhao, S. L., Huang, Y., McClements, D. J., Liu, X. B., Wang, P. J., & Liu, F. G. (2022). Improving pea protein functionality by combining high-pressure homogenization with an ultrasound-assisted Maillard reaction. *Food Hydrocolloids, 126*, Article 107441. https://doi.org/10.1016/j.foodhyd.2021.107441